Int. J. Heat Mass Transfer. Vol. 12, pp. 147–154. Pergamon Press 1969. Printed in Great Britain

THE EFFECT OF SUPERHEATING ON CONDENSATION HEAT TRANSFER IN A FORCED CONVECTION BOUNDARY LAYER FLOW

W. J. MINKOWYCZ† and E. M. SPARROW‡

(*Received* 29 *February* 1968 *and in revised form* 13 *May* 1968)

Abstract—An analysis of forced convection film condensation on a flat plate is performed for the case in which the free stream vapor flow is superheated. The solution method is applicable to free stream flows that are either binary mixtures of a condensable vapor and a noncondensable gas or pure condensable vapors. Specific numerical results are obtained for the condensation of steam with air as noncondensable. The effect of superheating on condensation heat transfer is found to be significant only in the range of relatively small differences between the free stream saturation temperature and the wall temperature. Furthermore, the influence of superheating is markedly augmented by the presence of noncondensable gases. Comparison of the present results for forced convection condensation with those for gravity-flow condensation indicates that the latter is much more sensitive to superheating.

NOMENCLATURE

c_p,	specific heat at constant pressure;
D,	binary diffusion coefficient;
F,	dimensionless stream function, equation (1b);
f,	dimensionless stream function, equation (1a);
h_{fg},	latent heat of condensation;
k,	thermal conductivity;
M,	molecular weight;
$\dot{m}$,	interface mass flux;
Pr,	Prandtl number, $c_p\mu/k$;
p,	total pressure;
p_v,	vapor pressure;
q,	surface heat flux/time-area;
R,	property ratio, $[(\rho\mu)_L/(\rho\mu)]^{\frac{1}{2}}$;
Sc,	Schmidt number, ν/D;
T,	temperature;
U_∞,	free stream velocity;
u, v,	velocity components;
W,	mass fraction of noncondensable;
x, y,	coordinates.

Greek symbols

δ,	condensate layer thickness;
η,	similarity variable, equation (1a);
η_δ,	value of η at $y = \delta$;
Θ,	dimensionless temperature, $(T - T_\infty)/(T_i - T_\infty)$;
θ,	dimensionless temperature, $(T - T_w)/(T_i - T_w)$;
μ,	absolute viscosity;
ν,	kinematic viscosity;
ξ,	similarity variable, equation (1b);
ρ,	density;
τ,	shear stress;
Φ,	mass fraction variable, $(W - W_\infty)/(W_i - W_\infty)$;
Ψ, ψ,	stream functions.

Subscripts

g,	gas;
i,	interface;
L,	condensed liquid;
sat, ∞,	free stream saturation;

† Department of Energy Engineering, University of Illinois of Chicago Circle, Chicago, Illinois, U.S.A.

‡ Coordenação dos Programas Pós-graduados de Engenharia, Universidade do Brasil, Rio de Janeiro, Brasil.

v, vapor;
w, wall;
∞, free stream;
mixture properties are unsubscripted.

Superscript
*, in the absence of superheating.

INTRODUCTION

FILM condensation in a laminar forced-convection boundary layer has been investigated for free stream flows consisting either of a pure saturated vapor [1–6] or of a saturated mixture of condensable vapor and noncondensable gas [3, 7]. On the other hand, the effect of vapor superheating on the condensation heat-transfer rate has, apparently, yet to be examined. While it may be anticipated that the heat transfer corresponding to condensation of a pure vapor is little affected by superheating, results for gravity-induced flow indicate [8] that the influence of superheating is substantially augmented by the presence of noncondensables.

The present investigation is aimed at determining the effect of vapor superheating on the surface heat flux for laminar forced-convection film condensation on a flat plate. A solution method is developed which is applicable to any binary mixture of condensable vapor and noncondensable gas and to any degree of superheating; the pure condensable vapor is included as a special case. Specific application is made to the situation in which the free stream flow is a mixture of steam and air. Heat-transfer results are obtained and presented for wide ranges in the free stream saturation temperature (i.e. pressure level), vapor superheat, air concentration, and stream-to-wall temperature difference.

The analytical model (see inset of Fig. 1) envisions the flow as consisting of a thin liquid layer adjacent to the plate and external boundary layers of velocity, temperature, and concentration in the vapor–gas mixture. The interface between the liquid and vapor–gas regions is a saturation state. The transport phenomena in the two regions are coupled by various conditions of continuity at the interface and by the constraint that the interface is impermeable to the noncondensable gas.

The present analysis is an extension of that reported in [7] and, aside from modifications appropriate to superheating, the analytical models are the same. To achieve a concise presentation here, liberal use will be made of the formulation and the results reported in the reference. For the benefit of readers who are interested in a detailed presentation of the present research, the authors have prepared a full-length report [9] which is available on request.

ANALYSIS AND SOLUTION

The formulation of the problem involves the successive analysis of the velocity, temperature, and concentration fields, the solutions to which facilitate the evaluation of the energy continuity condition at the interface. The thus-evaluated energy balance, taken in conjunction with saturation state data, is then employed in the simultaneous determination of the interface temperature and the thickness of the condensation film. Once this information is available, the heat-transfer results follow directly.

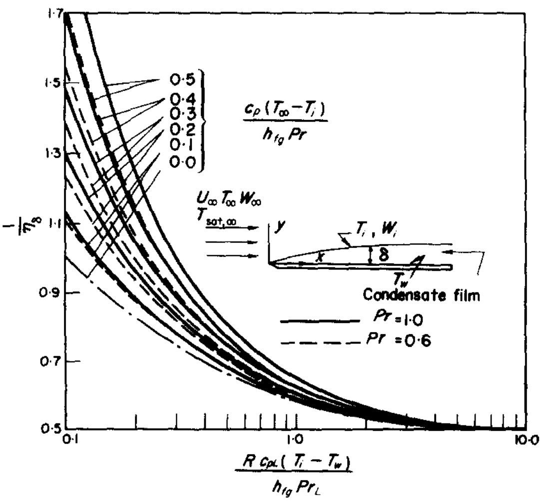

FIG. 1. Condensate layer thickness.

Velocity

The starting point for the analysis of the velocity field is the continuity and boundary-layer momentum equations. These equations are written for both the condensate layer and the vapor–gas boundary layer, along with appropriate boundary conditions at the plate surface and in the free stream. Coupling is provided by conditions of continuity at the interface.

The solution for the velocity field is facilitated by the use of similarity transformations, which are

$$\eta = y\sqrt{(U_\infty/\nu_L x)},\quad \psi = \sqrt{(U_\infty \nu_L x)}\, f(\eta), \qquad 0 \leqslant y \leqslant \delta \qquad (1a)$$

and

$$\xi = (y-\delta)\sqrt{(U_\infty/\nu x)},\quad \Psi = \sqrt{(U_\infty \nu x)}\, F(\xi), \qquad y \geqslant \delta \qquad (1b)$$

respectively for the liquid layer and the vapor–gas boundary layer. The properties of the liquid are distinguishable by the subscript L, while the properties of the vapor–gas mixture are unsubscripted. The location of the interface $y = \delta$ is alternatively designated as

$$\eta_\delta = \delta\sqrt{(U_\infty/\nu_L x)} \qquad \text{or} \qquad \xi = 0. \qquad (2)$$

The details of the velocity solution are presented in [7, 9]. For present purposes, it is sufficient to draw upon certain specific information provided by the solution. One useful finding is that the local condensation rate $\dot{m}$ (that is, the mass crossing the interface per unit time and unit area) is

$$\dot{m} = \tfrac{1}{2}\sqrt{(\rho\mu U_\infty/x)}\, F(0). \qquad (3)$$

$F(0)$ can therefore be regarded as a measure of the condensation rate. A second useful result is that η_δ, the dimensionless condensate layer thickness [see equation (2)], is a universal function of $F(0)$. The relationship between η_δ and $F(0)$ is listed in Table 1.

The just-cited information will be employed later in the analytical and numerical evaluation of the interface energy balance.

Table 1. Results from the velocity, temperature, and diffusion solutions

$F(0)$	$1/\eta_\delta$	$-\Theta'(0)$ or $-\Phi'(0)$ for Pr or Sc =							W_∞/W_i ($Sc = 0{\cdot}55$)
		0·55	0·6	0·7	0·8	0·9	1·0	1·1	
0·0500	1·8715	0·2791	0·2885	0·3059	0·3218	0·3365	0·3503	0·3632	0·9507
0·1000	1·3577	0·2898	0·3001	0·3192	0·3368	0·3533	0·3687	0·3833	0·9051
0·1500	1·1362	0·3005	0·3117	0·3326	0·3520	0·3701	0·3873	0·4036	0·8627
0·2000	1·0076	0·3113	0·3234	0·3461	0·3672	0·3872	0·4061	0·4242	0·8233
0·2500	0·9221	0·3221	0·3351	0·3596	0·3826	0·4044	0·4251	0·4451	0·7866
0·3000	0·8605	0·3330	0·3469	0·3733	0·3981	0·4217	0·4443	0·4661	0·7523
0·3500	0·8139	0·3439	0·3588	0·3870	0·4137	0·4392	0·4637	0·4874	0·7201
0·4000	0·7772	0·3549	0·3707	0·4008	0·4294	0·4568	0·4833	0·5089	0·6900
0·4500	0·7476	0·3659	0·3826	0·4147	0·4453	0·4746	0·5030	0·5305	0·6618
0·5000	0·7231	0·3769	0·3946	0·4287	0·4612	0·4925	0·5228	0·5524	0·6352
0·6000	0·6849	0·3991	0·4188	0·4568	0·4933	0·5286	0·5630	0·5966	0·5865
0·7000	0·6567	0·4214	0·4431	0·4852	0·5258	0·5652	0·6037	0·6415	0·5432
1·0000	0·6037	0·4894	0·5173	0·5719	0·6252	0·6774	0·7289	0·7797	0·4380
1·5000	0·5614	0·6053	0·6442	0·7209	0·7965	0·8713	0·9454	1·0192	0·3186
2·0000	0·5407	0·7244	0·7747	0·8744	0·9733	1·0716	1·1694	1·2670	0·2408
3·0000	0·5216	0·9698	1·0438	1·1913	1·3385	1·4854	1·6321	1·7789	0·1493
4·0000	0·5133	1·2229	1·3213	1·5179	1·7144	1·9109	2·1074	2·3041	0·1005
5·0000	0·5089	1·4813	1·6043	1·8505	2·0968	2·3433	2·5900	2·8368	0·0717
6·0000	0·5064	1·7427	1·8908	2·1871	2·4836	2·7803	3·0772	3·3743	0·0532
10·0000	0·5024	2·8110	3·0593	3·5563	4·0537	4·5514	5·0492	5·5472	0·0217

Temperature

As discussed in [7], the energy transport in the condensate layer is dominated by heat conduction for realistic values of the governing parameters,† so that the temperature profile is a straight line, that is,

$$(T - T_w)/(T_i - T_w) = \eta/\eta_\delta, \qquad \eta \leqslant \eta_\delta \quad (4)$$

wherein both the interface temperature T_i and the condensate layer thickness η_δ remain to be determined. For the vapor–gas region, consideration must be given to the complete layer energy equation

$$u\frac{\partial T}{\partial x} + v\frac{\partial T}{\partial y} = \frac{k}{\rho c_p}\frac{\partial^2 T}{\partial y^2} \quad (5)$$

which becomes, after application of the similarity transformation (1b)

$$\theta'' + \tfrac{1}{2}Pr\,F\theta' = 0 \quad (6)$$

in which $\theta(\xi) = (T - T_\infty)/(T_i - T_\infty)$ and Pr is the Prandtl number. The boundary conditions are $\theta(0) = 1$, $\theta(\infty) = 0$.

The solution for θ may be expressed in terms of integrals involving the known function $F(\xi)$.‡ Of particular relevance to the present investigation is the temperature derivative $\theta'(0)$ at the interface, the expression for which is

$$\Theta'(0) = -1 \Bigg/ \int_0^\infty \exp\left(-\frac{Pr}{2}\int_0^\xi F\,d\xi\right) d\xi. \quad (7)$$

The velocity function $F(\xi)$ depends parametrically on $F(0)$, and so does $\Theta'(0)$. Numerical values of $\Theta'(0)$, evaluated from equation (7), are listed in Table 1 as a function of $F(0)$ for several Prandtl numbers. As will be subsequently apparent [equation (9a)], the magnitude of the heat conducted to the interface from the vapor–gas region is proportional to $\Theta'(0)$ as well as to the temperature difference $(T_\infty - T_i)$.

† The role of energy conversion (subcooling) for gravity-flow condensation is discussed in [10–12].

‡ The simplicity of the solution for θ is a consequence of the constant property assumption.

Concentration

When a noncondensable gas is present in the free stream, it is well established that the dynamics of the condensation process gives rise to a build-up in the concentration of the noncondensable at the interface. The concentration of the noncondensable will be characterized here by its mass fraction $W(= \rho_g/\rho)$. The distribution of the mass fraction W within the boundary layer is governed by equation (5), in which T and $k/\rho c_p$ are respectively replaced by W and D (the binary diffusion coefficient). Moreover, by defining $\Phi = (W - W_\infty)/(W_i - W_\infty)$, equation (6) and its boundary conditions also apply for the concentration problem provided that Pr is replaced by the Schmidt number Sc. Consequently, the interfacial derivative $\Phi'(0)$ is given by the right-hand side of equation (7) with Sc replacing Pr. Thus, the listing of $\Theta'(0)$ values in Table 1 is also a listing of $\Phi'(0)$ values.

The quantity W_∞, representing the mass fraction of the noncondensable in the free stream, is one of the prescribed conditions of the problem. On the other hand, the interfacial mass fraction W_i is not known *a priori*. The determination of W_i is based on the fact that the interface is impermeable to the noncondensable. When this principle is expressed in mathematical terms, there follows [7]

$$\frac{W_\infty}{W_i} = 1 + \frac{F(0)Sc}{2\Phi'(0)}. \quad (8)$$

For a given Schmidt number, $\Phi'(0)$ is a function of $F(0)$ alone and, consequently, so is W_∞/W_i. With the forthcoming application to the steam–air system in mind, W_∞/W_i values have been listed in Table 1 (last column) for $Sc = 0{\cdot}55$. It is evident that for a given W_∞, there is a steady increase in W_i as the condensation rate $F(0)$ increases.

Energy continuity at the interface

As a final physical constraint, it is required that at the interface, the energy liberated as latent heat plus that conducted from the vapor–gas boundary layer be equal to the heat conducted into the condensate layer, that is

$$\dot{m}h_{fg} + k\partial T/\partial y = (k\partial T/\partial y)_L \tag{9}$$

which becomes, in terms of the variables of the analysis

$$\frac{F(0)}{2} = R\frac{c_{pL}(T_i - T_w)}{h_{fg}Pr_L}\frac{1}{\eta_\delta} - \frac{c_p(T_i - T_\infty)}{h_{fg}Pr}\Theta'(0) \tag{9a}$$

where $R = [(\rho\mu)/(\rho\mu)_L]^{\frac{1}{2}}$. The fluid properties appearing in equation (9a) will be evaluated at interfacial conditions.

Equation (9) is a relationship between the interface temperature T_i and the condensation rate $F(0)$, or alternatively, between T_i and the condensate layer thickness η_δ. This relationship is shown in Fig. 1, where $1/\eta_\delta$ is plotted as a function of $R[c_{pL}(T_i - T_w)/h_{fg}Pr_L]$ for parametric values of $c_p(T_\infty - T_i)/h_{fg}Pr$ and for two mixture Prandtl numbers, 0·6 and 1·0. The abscissa is a measure of the condensation rate, while the curve parameter is an index of the extent of the superheating. The figure shows that the effect of superheating on the thickness of the condensate layer is significant only at low condensation rates. When the condensation rate is large, the layer thickness is very little affected by superheating.

It will now be demonstrated that a second relationship between the unknowns is provided by the saturation state data for the condensing vapor. This information, usually available in the form of vapor pressure versus temperature, may also be represented in the form T_i as a function of W_i. On the other hand, W_i is a function of $F(0)$ for a given Schmidt number. Thus, there emerges a relationship between T_i and $F(0)$.

In the functional dependence of $\Theta'(0)$ and W_∞/W_i on $F(0)$, Pr and Sc respectively appear as parameters. It is proposed to evaluate these groups at the average of their values at the interface and in the free stream.

Computation of T_i and η_δ

In specifying the problem, it is reasonable to regard T_∞, $T_{\text{sat},\infty}$, W_∞, and T_w as known quantities. Among these, T_∞ and $T_{\text{sat},\infty}$ are, respectively, the actual temperature and saturation temperature of the free stream flow. Once the participation fluids are specified, information on the appropriate thermodynamic and transport properties may also be regarded as known.

A computation scheme for determining T_i and η_δ will now be described. The first step is to calculate the total pressure p of the system. For this purpose, one uses the first of the following

$$\left.\begin{aligned} \frac{p}{p_v} &= \frac{1 - W(1 - M_v/M_g)}{1 - W}, \\ W &= \frac{1 - (p_v/p)}{1 - (p_v/p)(1 - M_v/M_g)} \end{aligned}\right\} \tag{10}$$

in which p_v is the vapor pressure corresponding to $T_{\text{sat},\infty}$ and W is equal to W_∞. Next a trial value of T_i is proposed. The corresponding vapor pressure p_v is found from the saturation state data, and W_i is evaluated from the second of equations (10). Also, the fluid properties are evaluated at interface conditions.

Then, use is made of the pre-established relationships of η_δ, $\Theta'(0)$, and W_∞/W_i as functions of $F(0)$. In view of the just-mentioned determination of W_i corresponding to the guessed T_i, η_δ and $F(0)$ can now be found. Next, one returns to equation (9a), numerically evaluates all other quantities, and solves for T_i. The output value of T_i is compared with the initial guess, and the computation is either terminated or continued depending on whether the difference falls inside or outside of a given tolerance. When the computation is terminated, the end result is T_i and η_δ.

The just-described computation scheme can be programmed for solution by an electronic computer, the program being facilitated by curve fitting of the input functions.

When the free stream is a pure vapor, then $T_i = T_{\text{sat},\infty}$. The trial and error aspects of the aforementioned computation can be circumvented and results such as those of Fig. 1 can be generated directly.

Heat transfer

The local heat flux q at the plate surface is evaluated using Fourier's law which, by making use of equations (1a) and (4), gives

$$q = k_L(T_i - T_w)\sqrt{(U_\infty/\nu_L x)}\,(1/\eta_\delta). \quad (11)$$

To highlight the effects of superheating, the heat-transfer results will be presented as a ratio q/q^*, where q and q^* are characterized by identical operating conditions, except that q includes superheating while q^* is for no superheating. Thus,

$$\frac{q}{q^*} = \frac{(T_i - T_w)}{(T_i^* - T_w)}\frac{(1/\eta_\delta)}{(1/\eta_\delta^*)}\left(\frac{k_L}{k_L^*}\right)\left(\frac{\nu_L^*}{\nu_L}\right)^{\frac{1}{2}}. \quad (12)$$

T_i^* and $1/\eta_\delta^*$ are evaluated by the same procedure as described above, with the one modification that the last term of equation (9a) is deleted altogether. The properties k_L and ν_L are evaluated at a reference temperature that is one-third of the way between the wall and interface temperatures. At high condensation rates, equation (12) simplifies inasmuch as $\eta_\delta \approx \eta_\delta^*$ (Fig. 1).

For condensation of a pure vapor, only the ratio $(1/\eta_\delta)/(1/\eta_\delta^*)$ remains on the right-hand side of equation (12). At high condensation rates, $q \approx q^*$.

CONDENSATION OF STEAM WITH AIR AS NONCONDENSABLE

Heat-transfer results for a free stream flow consisting of a mixture of steam and air have been evaluated† and are presented in Figs. 2–4, respectively for $T_{sat,\infty} = 212$, 150, and 80°F. Each figure is subdivided into five graphs, each of which corresponds to a different free stream mass fraction of air in the range $0 \leqslant W_\infty \leqslant 0{\cdot}10$. In turn, each graph contains three curves characterized by the degree of superheating ($T_\infty - T_{sat,\infty}$), to which has been assigned values of 100, 200, and 400°F.

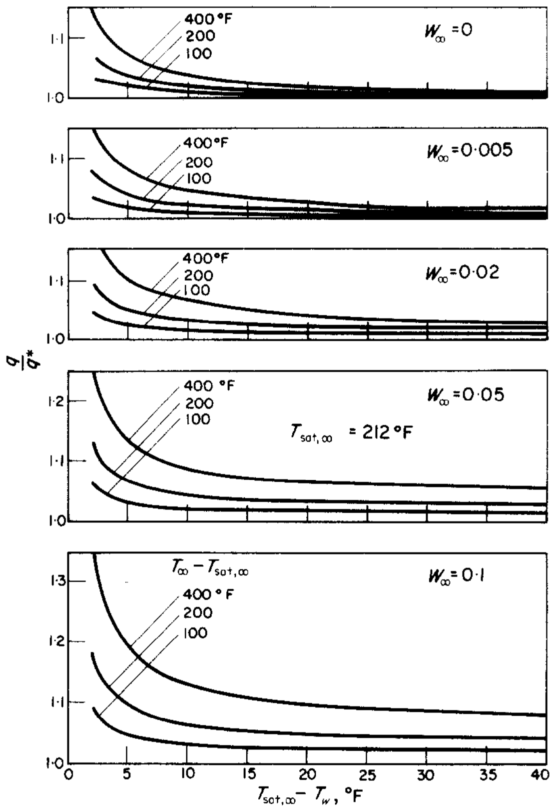

FIG. 2. Heat-transfer results, $T_{sat,\infty} = 212$°F.

The presentation of results gives the heat-transfer ratio q/q^* as a function of the temperature difference ($T_{sat,\infty} - T_w$). Inasmuch as q^* corresponds to the case of no superheating, it follows that the departures of the curves from unity provide a direct measure of the effect of superheating.

Inspection of the figures reveals that, as expected, the effect of superheating is to increase the surface heat transfer, such increases being accentuated at higher degrees of superheat. However, only in the range of very small ($T_{sat,\infty} - T_w$) are these increases large enough to be of marked practical interest. In this range, q/q^* is a strong function of ($T_{sat,\infty} - T_w$), and is also significantly affected by the level of the free

† The fluid properties employed in the evaluation are the same used in [8]. The Schmidt number was taken as 0·55.

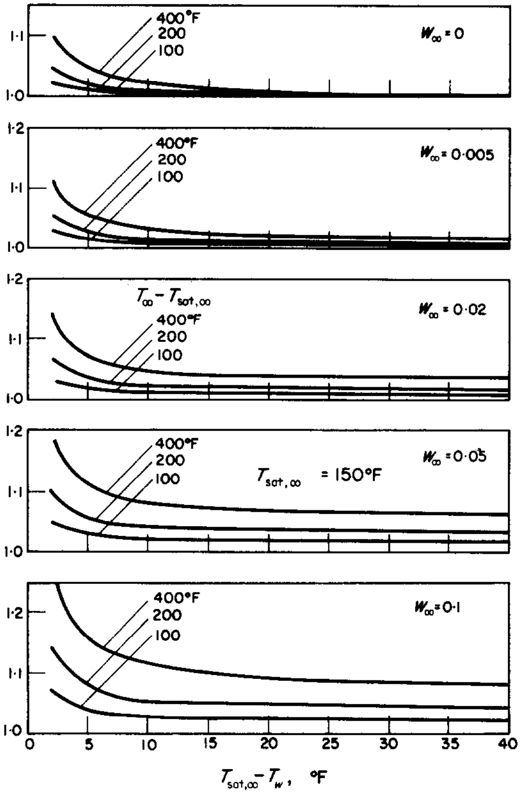

FIG. 3. Heat-transfer results, $T_{sat,\infty} = 150°F$.

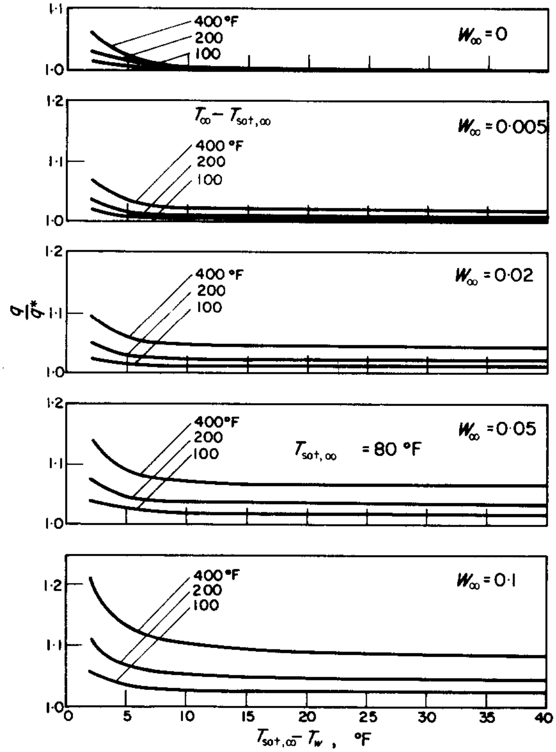

FIG. 4. Heat-transfer results, $T_{sat,\infty} = 80°F$.

stream saturation temperature and of the concentration of the noncondensable gas. The effects of superheating are most strongly manifested at higher $T_{sat,\infty}$ and W_∞.

For moderate and intermediate values of $(T_{sat,\infty} - T_w)$, the increases in the surface heat transfer due to superheating are less than 10 per cent. Moreover, q/q^* is relatively independent of $(T_{sat,\infty} - T_w)$ and is only slightly affected by $T_{sat,\infty}$ for fixed values of W_∞, $(T_\infty - T_{sat,\infty})$, and $(T_{sat,\infty} - T_w)$. For a small degree of superheating (say, 100°F), the deviations of q/q^* from unity are entirely negligible. A similar finding applies for condensation of a pure vapor, even at the largest degree of superheating examined here.

It is worthwhile to compare the present results with those for gravity-induced film condensation [8]. Such a comparison shows that condensation heat transfer in a forced convection boundary layer is much less affected by superheating than is gravity-induced condensation. A similar lesser sensitivity to the presence of noncondensable gases has also been demonstrated [7].

As a final remark, it may be noted that the q^* values (zero superheating) are available in [7].

CONCLUDING REMARKS

Experimental data on the effect of superheating on forced convection condensation appear to be presently unavailable in the published literature, thereby precluding a comparison between the present analysis and experiment. It is also appropriate to mention the analytical study of Koh [13], which came to the authors' attention in the latter stages of the present investigation. That publication describes a method for calculating the effect of superheating on forced convection condensation heat transfer;

but, aside from a single case, no heat transfer results are given. A fuller discussion of Koh's work appears on p. 1841 of [7], and the gist of that discussion continues to apply here.

REFERENCES

1. W. M. Rohsenow, J. H. Webber and A. T. Ling, Effect of vapor velocity on laminar and turbulent film condensation, *Trans. Am. Soc. Mech. Engrs* **78**, 1637 (1956).
2. R. D. Cess, Laminar film condensation on a flat plate in the absence of a body force, *Z. Angew. Math. Phys.* **11**, 426–433 (1960).
3. P. M. Chung, Film condensation with and without body force in a boundary layer flow of a vapor over a flat plate, NASA TN D-790 (1961).
4. J. C. Y. Koh, Film condensation in a forced-convection boundary layer flow, *Int. J. Heat Mass Transfer* **5**, 941–954 (1962).
5. I. G. Shekriladze and V. I. Gomelauri, Theoretical study of laminar film condensation of flowing vapor, *Int. J. Heat Mass Transfer* **9**, 581–591 (1966).
6. H. R. Jacobs, An integral treatment of combined body force and forced convection film condensation, *Int. J. Heat Mass Transfer* **9**, 637–648 (1966).
7. E. M. Sparrow, W. J. Minkowycz, and M. Saddy, Forced Convection condensation in the presence of noncondensables and interfacial resistance, *Int. J. Heat Mass Transfer* **10**, 1829–1845 (1967).
8. W. J. Minkowycz and E. M. Sparrow, Condensation heat transfer in the presence of noncondensables, interfacial resistance, superheating, variable properties, and diffusion, *Int. J. Heat Mass Transfer* **9**, 1125–1144 (1966).
9. W. J. Minkowycz and E. M. Sparrow, The effect of superheating on condensation heat transfer in a forced convection boundary layer flow, Technical Report No. 7, Department of Energy Engineering, University of Illinois at Chicargo Circle (1967).
10. W. M. Rohsenov, Heat transfer and temperature distribution in laminar film condensation, *Trans. Am. Soc. Mech. Engrs* **78**, 1645–1648 (1956).
11. J. C. Y. Koh, E. M. Sparrow, and J. P. Hartnett, The two-phase boundary layer in laminar film condensation, *Int. J. Heat Mass Transfer* **2**, 69–82 (1961).
12. H. R. Jacobs, An integral treatment of combined body force and forced convection in laminar film condensation, *Int. J. Heat Mass Transfer* **9**, 637–648 (1966).
13. J. C. Y. Koh, Laminar film condensation of condensable gases and gaseous mixtures on a flat plate, in *Proceedings of the Fourth National Congress of Applied Mechanics*, pp. 1327–1336. The American Society of American Engineers, New York (1962).

Abstract—Une analyse de la condensation par film en convection forcée sur une plaque plane est effectuée dans le cas où l'écoulement de vapeur dans l'écoulement libre est surchauffé. La méthode de résolution est appliquable aux écoulements libres qui sont, soit des mélanges binaires d'une vapeur condensable et d'un gaz non condensable, soit des vapeurs pures condensables. Les résultats numériques spécifiques sont obtenus pour la condensation de la vapeur d'eau avec l'air comme gaz non condensable. L'effet de la surchauffe sur le transport de chaleur par condensation est sensible seulement dans une gamme de différences relativement faibles avec la température de saturation de l'écoulement libre. De plus, l'influence de la surchauffe est augmentée notablement par la présence de gaz non condensables.

La comparaison des résultats actuels pour la condensation par convection forcée avec ceux pour la condensation avec écoulement sous l'effet de la gravité indique que cette dernière est beaucoup plus sensible à la surchauffe.

Zusammenfassung—Filmkondensation an der ebenen Platte wird theoretisch untersucht. Dabei wird der Fall betrachtet, dass der Dampfstrom überhitzt ist und dass der Kondensatabfluss durch die Dampfströmung erzwungen wird. Die dargestellte Lösungsmethode lässt sich für reine Dämpfe und für Inertgas enthaltende Dämpfe anwenden. Numerische Ergebnisse werden für die Kondensation von Dampf mit Luft als Inertgas erhalten. Ein starker Einfluss der Überhitzung zeigt sich nur bei kleinen Differenzen zwischen der Sättigungstemperatur des Dampfstromes und der Wandtemperatur.

Der Einfluss der Überhitzung wird wesentlich verstärkt durch die Anwesenheit von Inertgasen. Ein Vergleich der Ergebnisse zwischen dem durch die Dampfströmung erzwungenen Kondensatabfluss und dem durch Schwerkraft erzwungenen zeigt, dass letzterer einer Überhitzung gegenüber empfindlicher reagiert.

Аннотация—Выполнен анализ пленочной конденсации на плоской пластине при вынужденной конвекции для случая, когда свободная струя пара является перегретой. Метод решения можно применить к свободным струям, представляющим собой или бинарные смеси конденсируемого пара и неконденсируемого газа или чистых конденсируемых паров. Получены частные численные результаты при конденсации пара в неконденсируемом воздухе. Найдено, что перегрев значительно влияет на теплообмен при конденсации только при сравнительно небольших отклонениях от температуры насыщения свободного потока. Кроме того, влияние перегрева заметно усиливается при наличии неконденсируемых газов. Сравнение результатов конденсации в условиях вынужденной конвекции с данными по конденсации при естественной конвекции обнаруживает, что при естественной конвекции перегрев оказывает большее влияние.